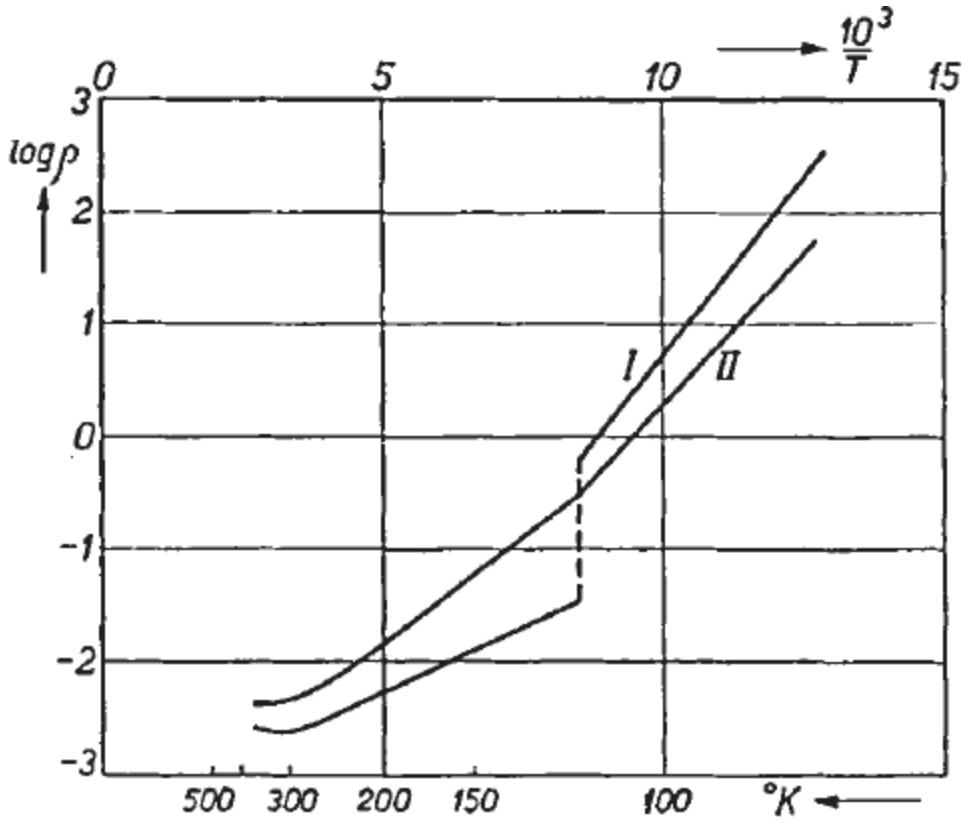

We thought it possible that the statistical distribution of Fe^{2+} and Fe^{3+}, which is a statistical distribution of electrons about the double number of lattice points containing Fe^{3+}, and which accounts for the rather high electronic conductivity of magnetite, would lead to some type of order at lower temperatures. A transition of this kind would probably offer an explanation of the anomalies at 120° K. One

The so-called Verwey transition in Fe_3O_4 [Nature **144** (1939) 327].

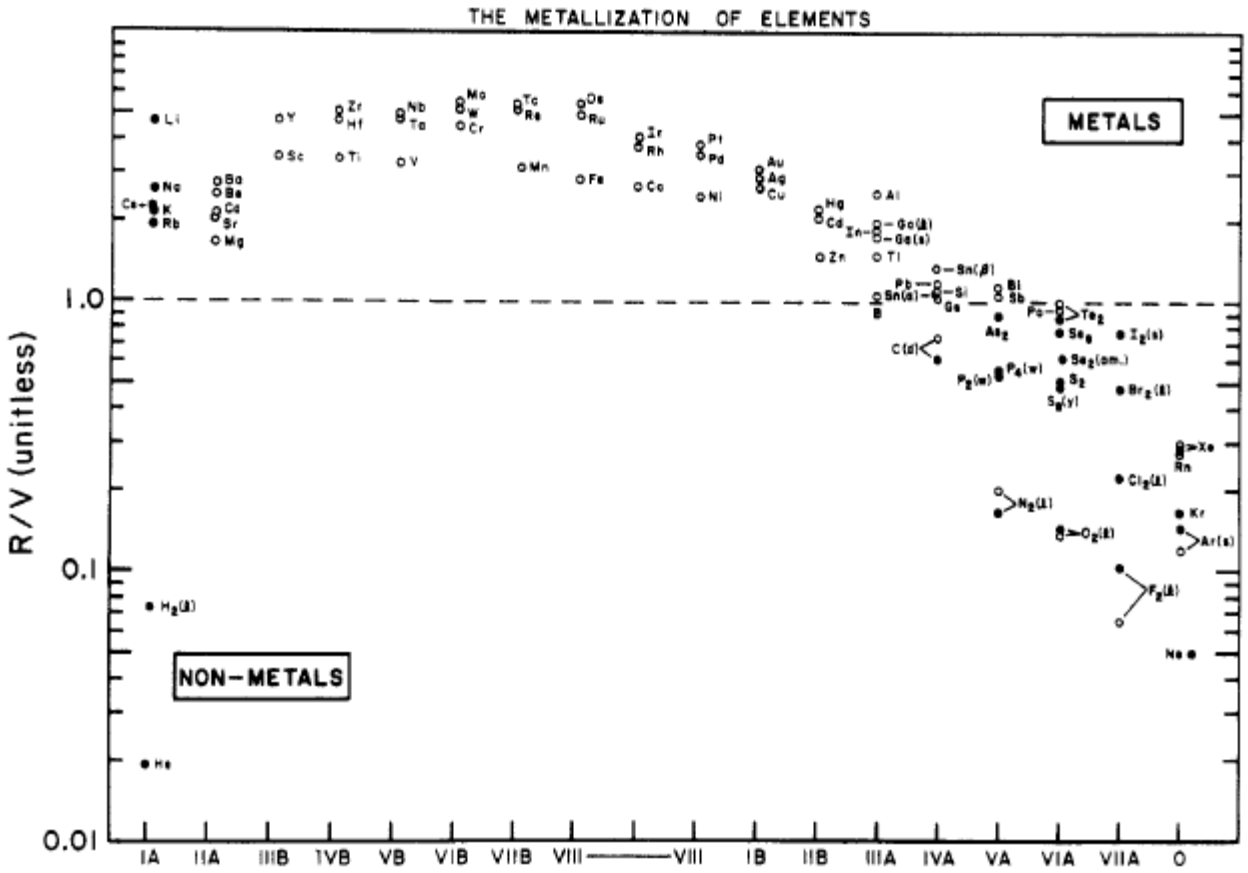

Figure 1. Metallization of elements under the ambient conditions imposed on this planet. The figure shows the ratio (R/V) for elements of the s, d, and p blocks of the periodic table. Here R is the molar refractivity and V is the molar volume; see text. The shaded circles represent elements for which both R and V are known experimentally. The open circles are for elements of which only V is known experimentally, and R is calculated. Taken from ref 2.

The Clausius-Mosotti equation gives (R is the molar refractivity and V is the molar volume:)

$$\frac{\varepsilon - 1}{\varepsilon + 2} = \frac{R}{V}$$

Metals have:

$$\varepsilon = \infty$$

P. P. Edwards and M. J. Sienko, *Acc. Chem. Res.* **15** (1982) 87-93

In a band theory of metals, systems with free electrons remain metallic no matter what the separation between the atoms (or no matter how low the density of electrons).

However, as the density of electrons, *n*, decreases, the screening of charges also decreases.

Thomas-Fermi:

$$U(r) = -(e^2/r)\exp(-qr);$$

$$q^2 = 4me^2(3n/\pi)^{1/3}/\hbar$$

This gives the Mott criterion:

$$n_c^{1/3} a_H^* \cong 0.25$$

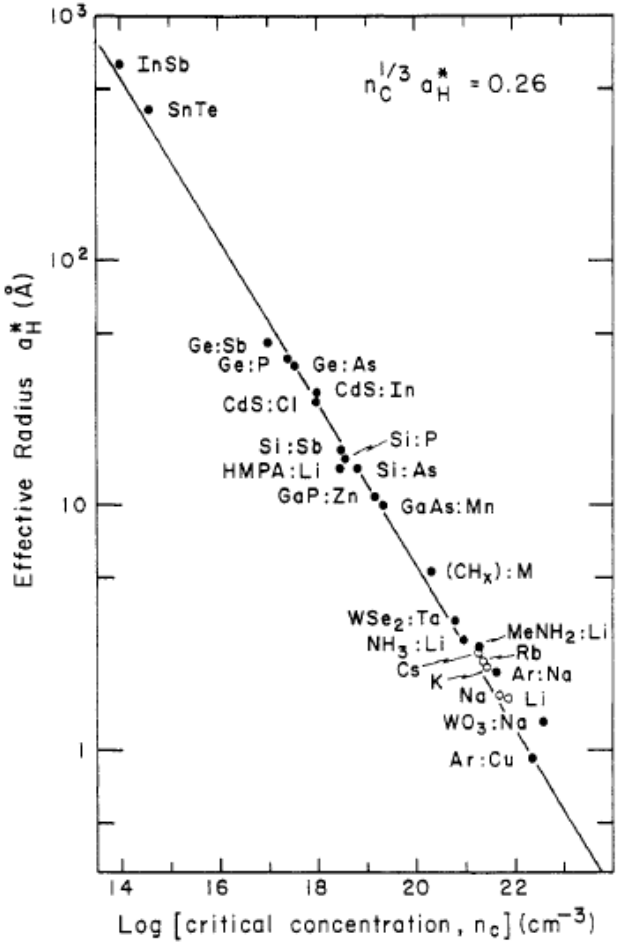

Figure 8. Transition to the metallic state. A logarithmic plot of the effective radius, a_H^*, of the localized-electron state vs. the critical concentration for metallization, n_c, in a variety of systems. Taken from ref 30.

P. P. Edwards and M. J. Sienko, *Acc. Chem. Res.* **15** (1982) 87-93

Examples:

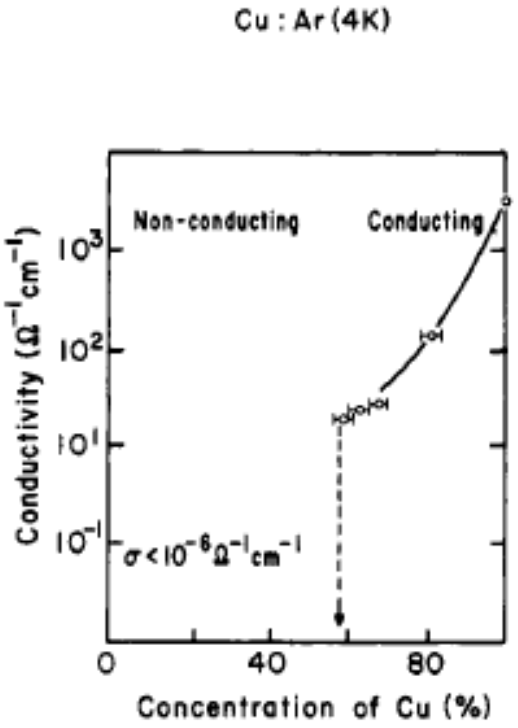

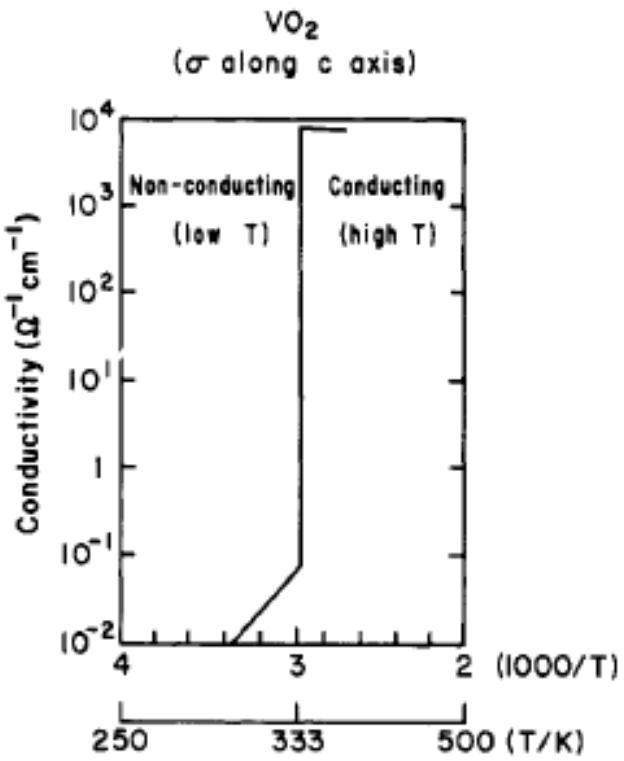

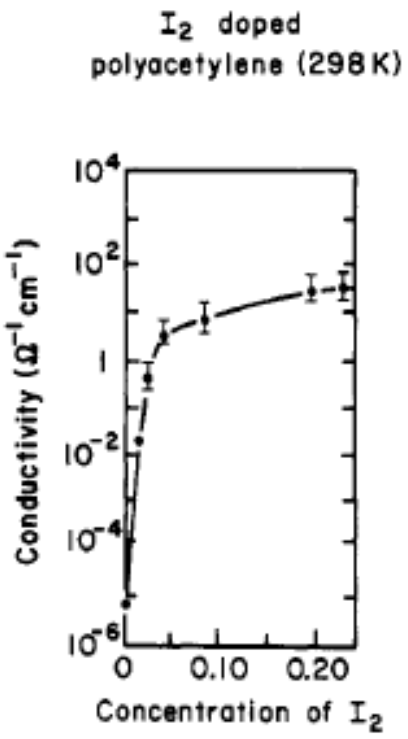

P. P. Edwards and M. J. Sienko, *Acc. Chem. Res.* **15** (1982) 87-93

The Hubbard model and the Zaanen-Sawatzky-Allen [*Phys. Rev. Lett.* **55** (1985) 418] phase diagram.

Mott-Hubbard:
$2V^{4+}O_2^{2-} \rightarrow V^{5+}O_2^{2-} + V^{3+}O_2^{2-}$

Charge-Transfer:
$Cu^{2+}O^{2-} \rightarrow Cu^{1+}O^{1-}$

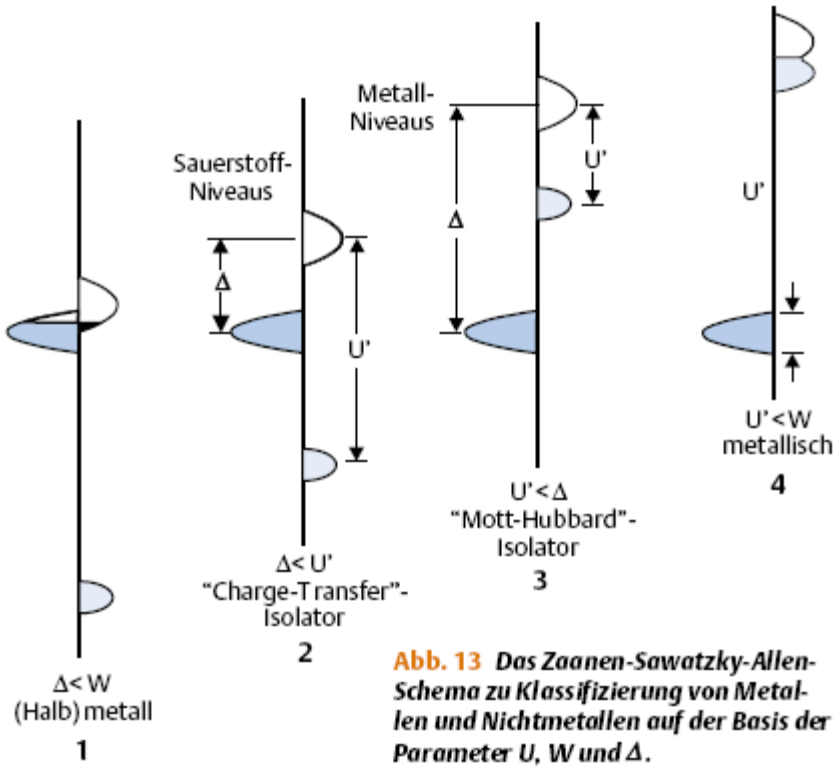

Abb. 13 ***Das Zaanen-Sawatzky-Allen-Schema zu Klassifizierung von Metallen und Nichtmetallen auf der Basis der Parameter U, W und Δ.***

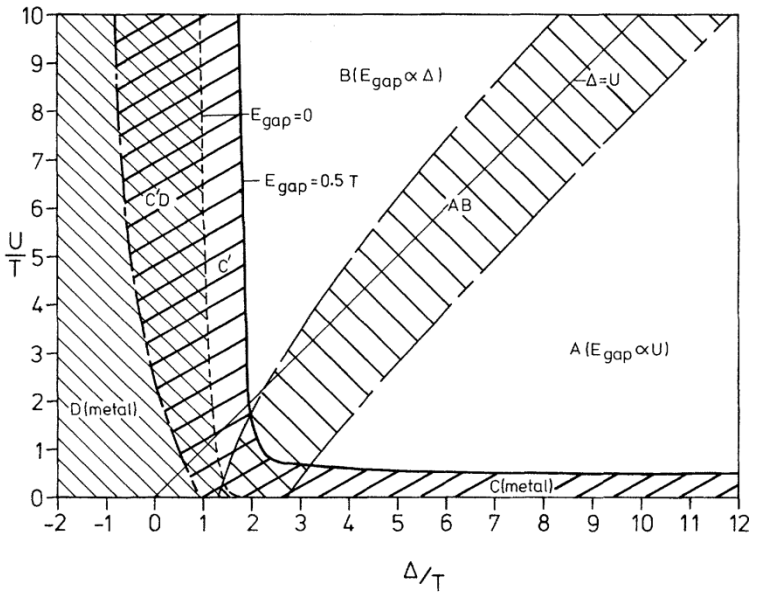

FIG. 3. A phase diagram exhibiting the various regions discussed in the text. The heavy solid line is the semiconductor-metal separation line.

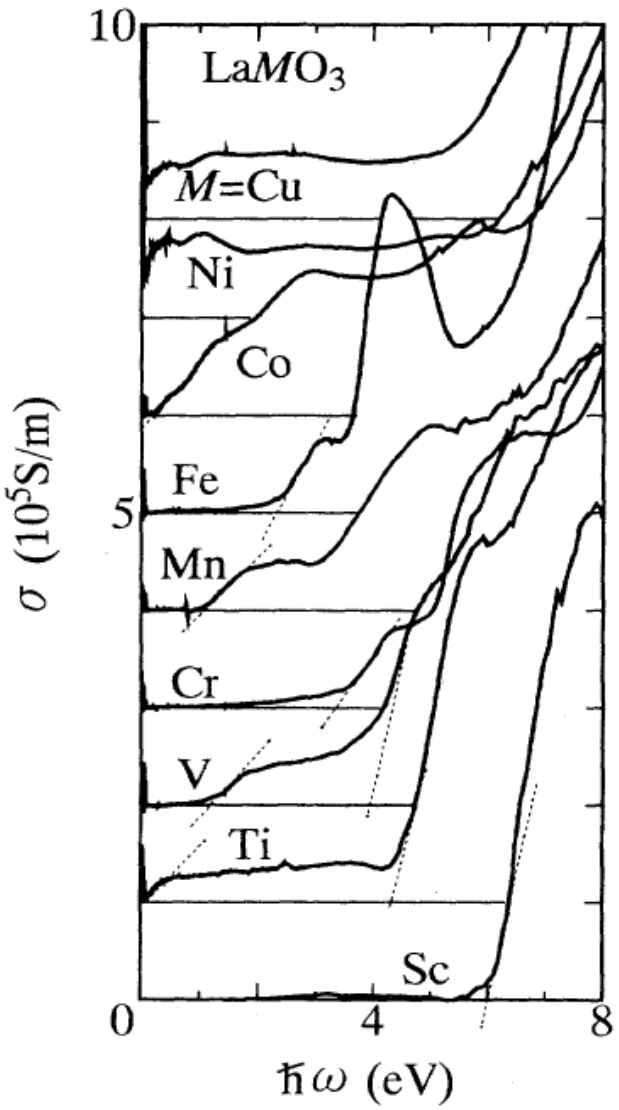

$LaMO_3$ perovskites: Band gaps from optical measurements.

Arima, Tokura, and Torrance, *Phys. Rev. B.* **48** (1993) 17006.

Class 6: Metal-insulator transitions

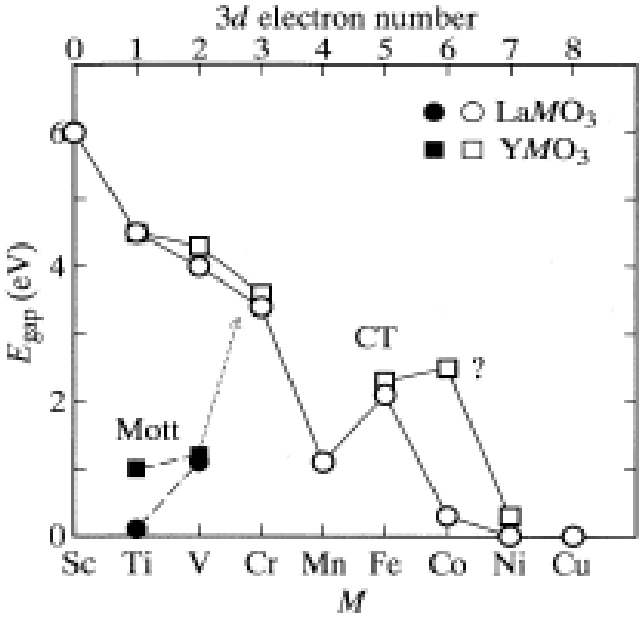

FIG. 2. Optical gap plotted against the 3*d* transition-metal element. Solid circles: Mott gap in $LaMO_3$. Solid squares: Mott gap in YMO_3. Open circles: CT gap in $LaMO_3$. Open squares: CT gap in YMO_3.

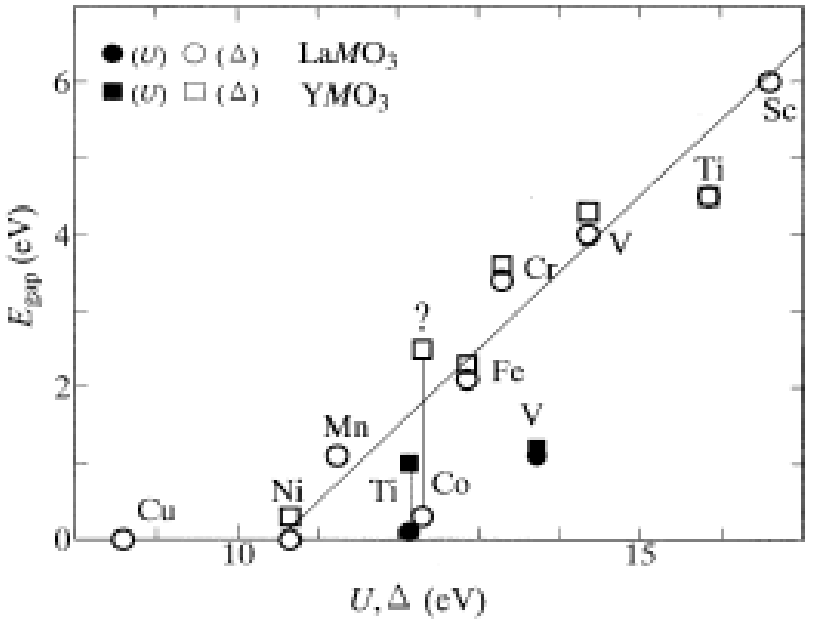

FIG. 3. The measured value of optical gap plotted against the calculated value based on the simple ionic model. Solid circles: Mott gap in $LaMO_3$. Solid squares: Mott gap in YMO_3. Open circles: CT gap in $LaMO_3$. Open squares: CT gap in YMO_3.

Arima, Tokura, and Torrance, *Phys. Rev. B.* **48** (1993) 17006.

Class 6: Metal-insulator transitions

VO_2

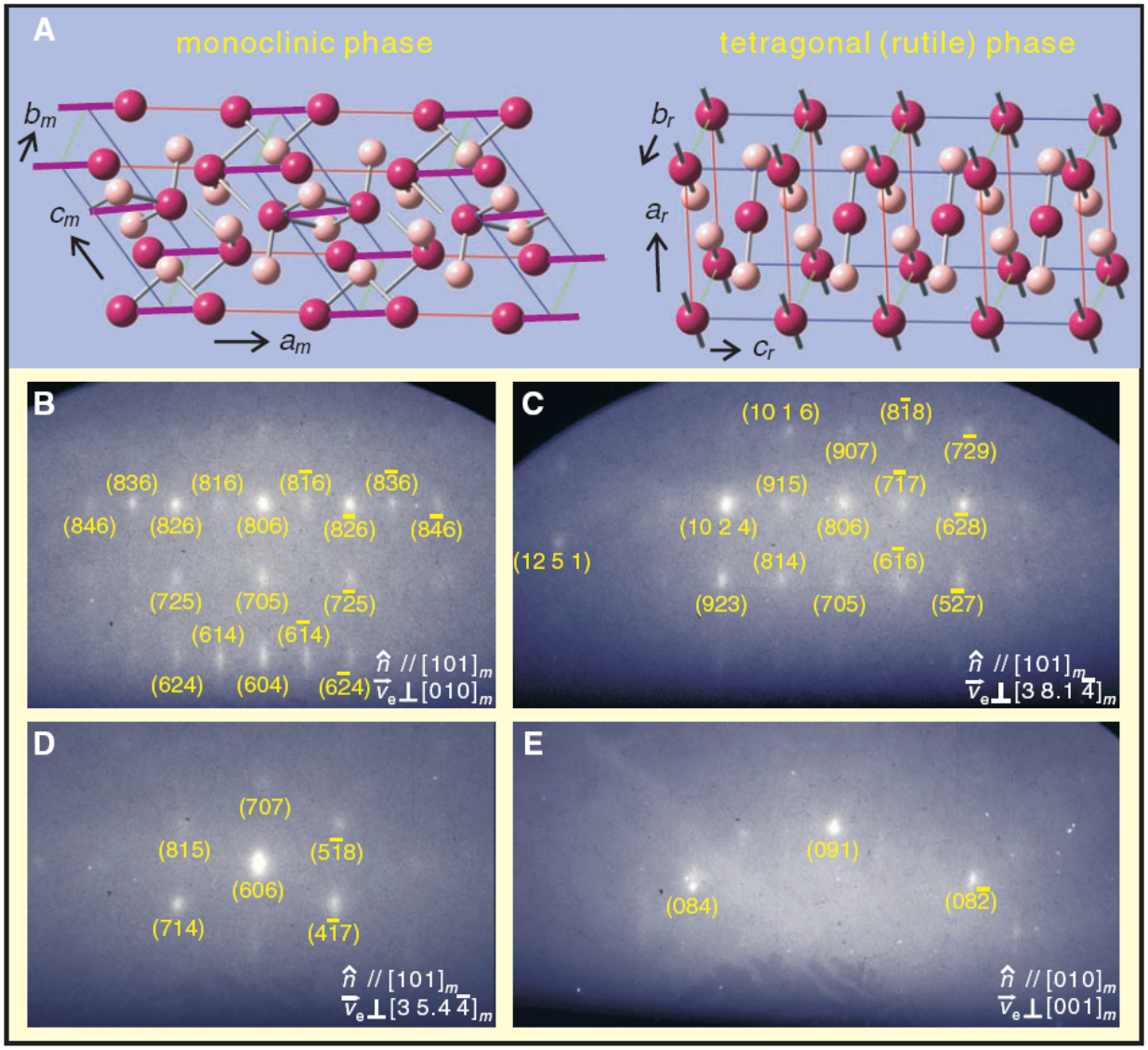

Fig. 1. Crystal structures of vanadium dioxide phases and observed Bragg diffraction. (**A**) Crystal structure of the monoclinic, low-temperature phase (left) and the rutile, high-temperature phase (right). Vanadium atoms are depicted in red and oxygen atoms in a lighter color. Because of a symmetry-breaking pairing of vanadium atoms (violet lines), the axis definitions change. Monoclinic coordinates and axes are used in the paper. (**B** to **E**) Typical diffraction patterns observed by ultrafast electron crystallography for different crystal surfaces and different zone axes; $\hat{n}$ is the surface normal direction and $\vec{v}_e$ is the electron direction (zone axis). All Bragg spots can be identified as the monoclinic structure (yellow labels).

Baum, Yang, Zewail, *Science* **318** (2007) 788.

Class 6: Metal-insulator transitions

VO_2

Fig. 2. Ultrafast, fs and ps, diffraction dynamics of the structural phase transition. (**A**) Intensity change of the (606) Bragg spot with time. A decay with a time constant τ_1 of 307 fs was obtained on the total time scale of ±3 ps (*40*); note the change in intensity of diffraction in the 250-fs steps. (**B**) Intensity change of (606) (blue) and (091) (red) spots with time. For all investigated Bragg spots, two different types of dynamics were observed: a femtosecond decay similar to the blue trace was measured for (806), (826), (8$\bar{2}$6), (846), (8$\bar{4}$6), (606), (714), (4$\bar{1}$7), (10 2 4), and (6$\bar{2}$8); a decay with a time constant τ_2 of 9.2 ps, similar to the red trace, was measured for (091), (084), and (0 8 $\bar{2}$), on the total time scale of 40 ps. The temporal range values (Δt_1 and Δt_2) over which the decay is pronounced are 760 fs and 15 ps (*40*). This difference indicates a stepwise mechanism for atomic motions.

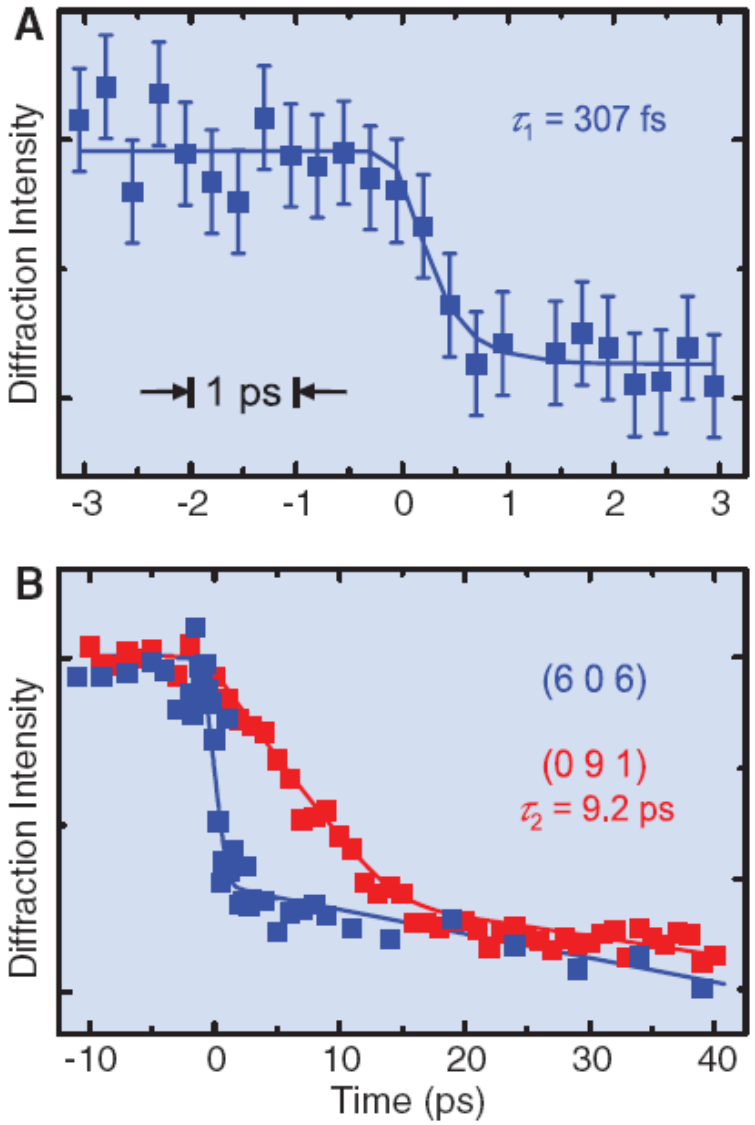

Baum, Yang, Zewail, *Science* **318** (2007) 788.

Class 6: Metal-insulator transitions

VO_2

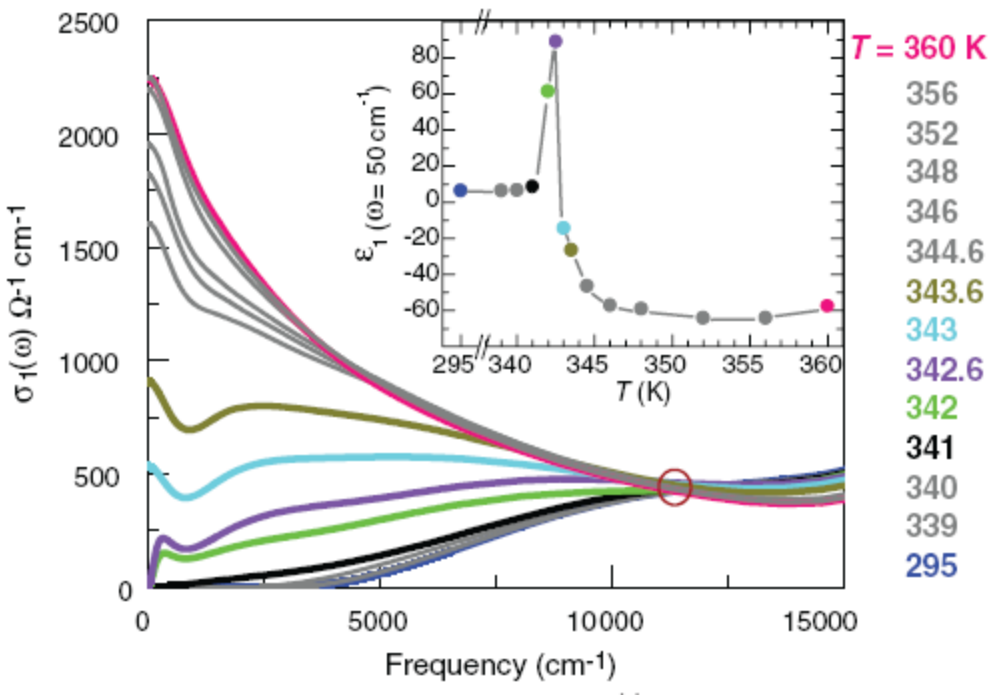

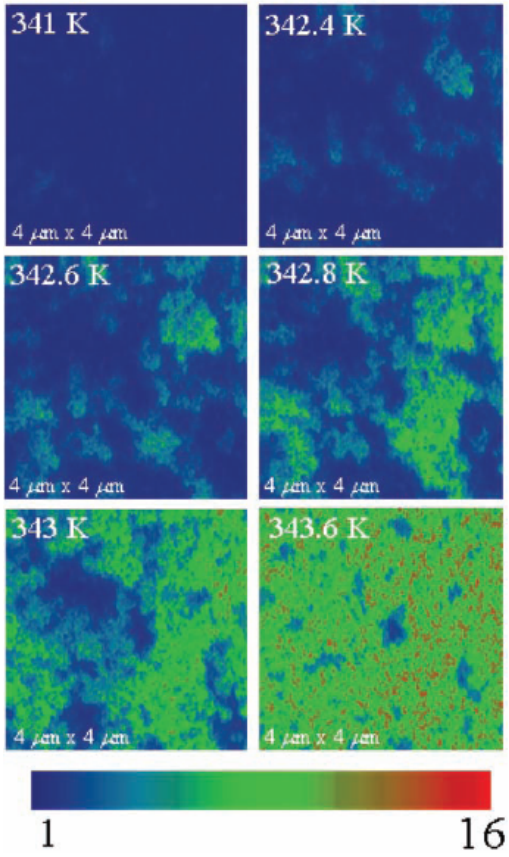

Fig. 2. Images of the near-field scattering amplitude over the same 4-μm-by-4-μm area obtained by s-SNIM operating at the infrared frequency ω = 930 cm^{-1}. These images are displayed for representative temperatures in the insulator-to-metal transition regime of VO_2 to show percolation in progress. The metallic regions (light blue, green, and red colors) give higher scattering near-field amplitude compared with the insulating phase (dark blue color). See (*13*) for details.

Basov and coworkers, *Science* **318** (2007) 1750.

Class 6: Metal-insulator transitions

VO_2

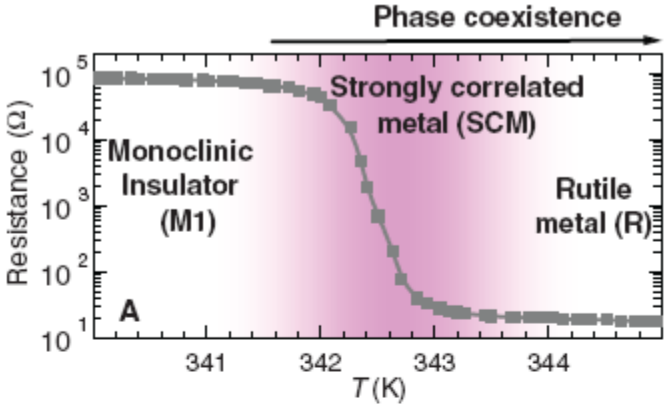

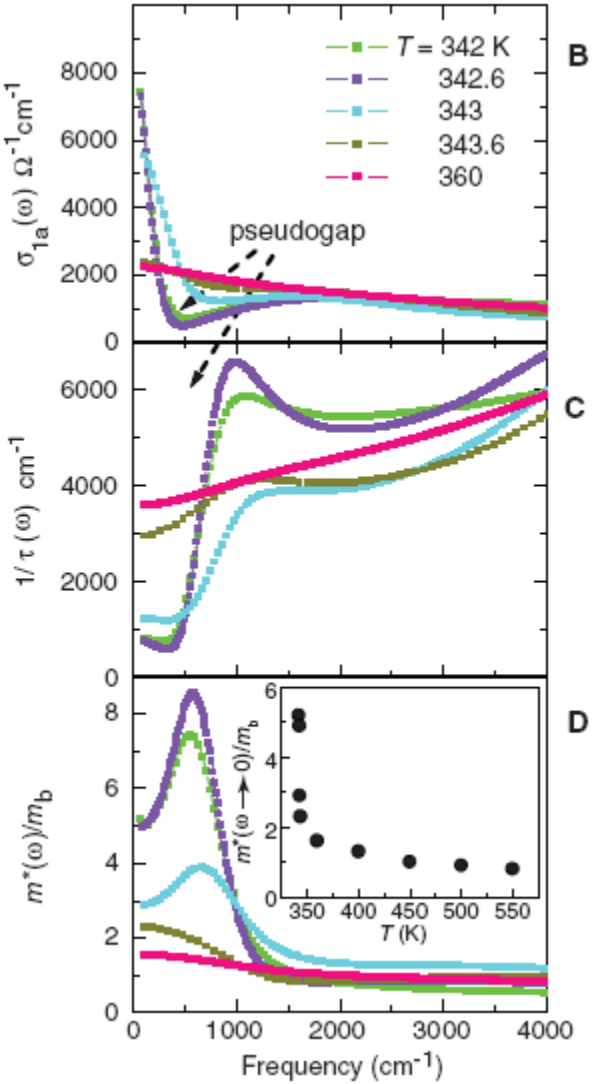

Fig. 3. (**A**) The phase diagram of VO_2 and the resistance-temperature curve showing the insulator-to-metal transition. The shaded area highlights the region of the phase diagram in which the strongly correlated metal (SCM) with divergent quasi-particle mass and an optical pseudogap exists. (**B** to **D**) The evolution of the optical conductivity $\sigma_{1a}(\omega)$, the scattering rate $1/\tau(\omega)$, and the optical effective mass normalized by the band value $m^*(\omega)/m_b$ of the metallic regions of VO_2 with increasing temperature. The inset in (D) shows the $\omega \rightarrow 0$ limit of the mass enhancement factor as a function of temperature. The data points between T = 400 K and 550 K are taken from (*22*).

Basov and coworkers, *Science* **318** (2007) 1750.